Article ID: 1000-324X(2017)04-0443-06 **DOI:** 10.15541/jim20160201

Influence of N Doping on the Electronic Structure and Absorption Spectrum of Ca_2SiO_4: Eu^{2+} Phosphor

CHEN Hai-Tao[1, 2], HUANG Xue-Fei[1], HUANG Wei-Gang[1]

(1. College of Material Science and Engineering, Sichuan University, Chengdu 610064, China; 2. College of Physics and Engineering, Chengdu Normal University, Chengdu 611130, China)

Abstract: The electronic structure and absorption spectrum of Ca_2SiO_4: Eu^{2+} was studied by using density functional theory. It is found that N atoms substituted provide many states around the Femi level, which leads to narrow optical band gap and interband transition originating from N2p to the Eu4f. In the N-doped Ca_2SiO_4: Eu^{2+} phosphor, Eu^{2+} ions experience a strong nephelauxetic effect and crystal field due to the coordinating nitrogen ions around the activated centers, which results in Eu4f and 5d states splitting. Thus, the red-shift of the absorption spectrum and high absorption band in the wavelength of 220–470 nm takes place for the N-doped Ca_2SiO_4: Eu^{2+} phosphor.

Key words: N-impurity; silicate phosphor; light emitting diodes (LEDs); density functional theory (DFT)

Rare earth (RE) doped silicate phosphors have applications in white light emitting diodes (white-LEDs) due to their low energy consumption, long lifetime and mercury free[1-3]. Divalent europium is more stable in an alkaline earth silicate host and more easily diffuses into the lattice sites because the ion radii of them are similar to each others[4–5]. On the other hand, it is well known that silicate material has good thermal and chemical stability. Thus, alkaline earth silicon compounds doped with divalent europium ions are good candidates for high effective luminescence phosphors and abundant color representation. In particular, Eu^{2+}-doped Ca_2SiO_4 phosphor has been considered as a green emitting material for white LED, pumped by ultraviolet-light[6].

Recently, our research group have been successfully synthesized some new nitrogen-contained solid solution green phosphors, such as $Ca_2Si(O_{4-x}N_x)$: Eu^{2+} and $Ca_2MgSi_2O_{7-x}N_x$: Eu^{2+}[7-8]. It was found that the $Ca_2Si(O_{4-x}N_x)$: Eu^{2+} phosphor can be efficiently excited at the wavelength of 270–400 nm and improves the intensity of luminescence significantly due to the N doping[7]. Though both β and γ phases of pure Ca_2SiO_4 crystallites are stable at room-temperature, β phase appears more stable in the case of Eu^{2+}-doped Ca_2SiO_4 phosphors. It is interesting to understand how nitrogen (N) atoms affect the electronic structure of β-Ca_2SiO_4: Eu^{2+} and improve its photoluminescence properties.

In recent years, it is demonstrated that the density functional theory (DFT) can satisfactorily provide detailed information on electronic properties of RE doped phosphors and the relationship with photoluminescence properties[9-13]. Therefore, this paper is to present a comprehensive study on the electronic structures of the N doped and un-doped β-Ca_2SiO_4: Eu^{2+} phosphors. Atomic populations, total density of states (TDOS) and partial density of states (PDOS) as well as absorption spectra of them are computed. Subsequently, the effects of N doping on the electronic properties and the absorption spectra of the phosphors are presented.

1 Theoretical simulation

The present calculations were performed based on DFT within the Cambridge Serial Total Energy Package (CASTEP) plane wave code[14]. In order to obtain accurate electronic structure, the method of total-energy functional (LDA+U) was adopted to overcome the well-known shortcoming of LDA. The ultrasoft pseudopotentials were used to describe the interaction of ionic core and valence electrons. Brillouin-zone integrations were performed using Monkhorst and Pack k-point meshes[15]. During the calculation, the 500 eV for cutoff energies and 2×3×2 for the numbers of k-point can ensure the convergence for the total energy. All the calculations were considered converged when the maximum force on the atom was below 0.003 eV/nm, maximum stress was below 0.05 GPa, and the maximum displacement between cycles was below 0.01 nm.

Received date: 2016-03-30; **Modified date:** 2016-06-27
Foundation item: National Natural Science Foundation of China (51401135); Foundation of Chengdu Normal University (YJRC2015-1)
Biography: CHEN Hai-Tao(1967–), male, professor, PhD. E-mail: chqcht@sina.com
Corresponding author: HUANG Wei-Gang, professor. E-mail: huangwg56@163.com

The β phase of Ca_2SiO_4 crystals has a trigonal structure with space group P21/n with the lattice constants a = 0.5502 nm, b = 0.6745 nm, c = 0.9297 nm and the crystal plane angles are $\alpha = \gamma = 90°$ and $\beta = 94.591°$. It is well known that Ca ions have two different sites in β-Ca_2SiO_4: Ca(1) with seven Ca–O and bonds 0.2 nm bonding length and Ca(2) with eight coordination and bonds 0.187 nm bonding length. Thus, it is generally accepted that the Eu atoms occupy both two Ca sites in the lattice[16]. Thus, a super-cell of β-Ca_2SiO_4 containing 84 atoms is firstly formed in which one Ca atom located at Ca(1) (or Ca(2)) position is replaced by one Eu atom, respectively, as shown in Fig. 1(a). Then, another super-cell of $Ca_2SiO_{3.75}N_{0.25}$: Eu^{2+} composed of 84 atoms is constructed, in which three O atoms are replaced by three N atoms (Fig. 1(b)).

2 Results and discussion

2.1 Mulliken population

The Mulliken atomic charges populations of Ca_2SiO_4: Eu^{2+} is shown in Table 1. It is easily seen that only O atoms own negative charges because of obtaining electrons. Meanwhile, Si, Ca and Eu atoms own positive charges because of losing electrons. Covalent bonds are localized between Si atoms and O atoms because Si atom possesses relative weak ability to lose electrons. On the other hand, Ca and Eu atoms form ionic bonds with O atoms due to their strong ability to lose electrons. Further more, it is Eu^{2+} not Eu^{3+} replacing one Ca^{2+} of $Ca_{24}Si_{12}O_{48}$ because seven electrons are localized in the 4f orbital of Eu ion in $Ca_{23}EuSi_{12}O_{48}$.

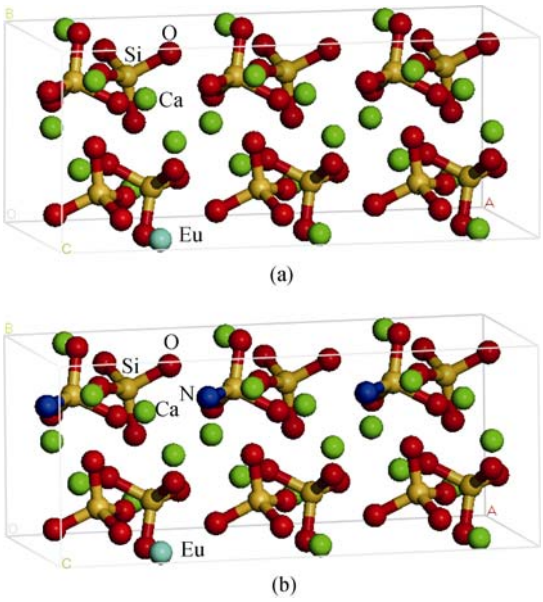

Fig. 1 Structure of the super-cell of Ca_2SiO_4: Eu^{2+} without (a) and with (b) substitution of N atoms for O atoms

Table1 Atomic populations of Ca_2SiO_4: Eu^{2+}

Case	Eu site	Element	s	p	d	f	Total
1	Ca(1)	O	1.88	5.31	0	0	7.19
		Si	0.68	1.50	0	0	2.18
		Ca	2.18	6.00	0.34	0	8.52
		Eu	2.17	6.24	0.67	7	16.07
2	Ca(2)	O	1.86	5.23	0	0	7.09
		Si	0.70	1.47	0	0	2.17
		Ca	2.14	6.00	0.60	0	8.74
		Eu	2.14	6.13	0.60	7	15.87

2.2 Band structures

For the case 1 in Table 1, the calculated band structures of N-doped and un-doped β-Ca_2SiO_4: Eu^{2+} are plotted in Fig. 2. In order to show the relationship between the band structures and their TDOS, the TDOS are also plotted here. It is seen from Fig. 2 that both the N-doped and un-doped Ca_2SiO_4: Eu^{2+} phosphors show direct optical band gaps, which is propitious to luminescence since the transition probability of the direct band gap is higher than that of the indirect band gap due to no phonons involved in the transition process[10]. The calculated band gap energy is 4.45 eV because the valence band maximum and conduction band minimum are 0 eV and 4.45 eV, respectively, at the G point of Brillouin zone in Fig. 2(a). When N atoms are doped, the calculated band gap energy is 0.644 eV, which is much smaller than that of Ca_2SiO_4: Eu^{2+}. The reason is that the partial substitution of N atoms for O atoms results in higher valence band and smaller band gap width. Besides, the labels of the energy bands (1, 2, 3, 4 and 5) and the interband transitions (a, b and c) obtained from the analysis of Fig. 4 are shown in the Fig. 2.

Figure 3 shows the calculated band structures and TDOS of the N-doped and un-doped β-Ca_2SiO_4: Eu^{2+} for the case of 2 in Table 1. It is seen in Fig. 3 that direct optical band gaps appear in the case 2, which is similar to the case 1 in Fig. 2. The valence band maximum and conduction band minimum are located at –0.01 eV and 4.66 eV in Fig. 3(a), respectively. Therefore, the calculated band gap energy is 4.67 eV.

As three O atoms are substituted by three N atoms in Fig. 3(b), the band gap energy is reduced to 0.807 eV. Therefore, the doping of N atoms leads to elevating the valence band maxim and narrowing the band gap. Besides, the labels of the energy bands (6, 7, 8, 9, 10 and 11) and the interband transitions (e, f and g) obtained from analysis of Fig. 5 are identified in Fig. 2.

2.3 Densities of states

Figure 4 shows the PDOS of the N-doped and un-dopedβ- Ca_2SiO_4: Eu^{2+} for the case 1, respectively. Only the top of the valence band and the bottom of the conduction band are shown in Fig. 4 because the optical absorption is mainly determined by the states close to the

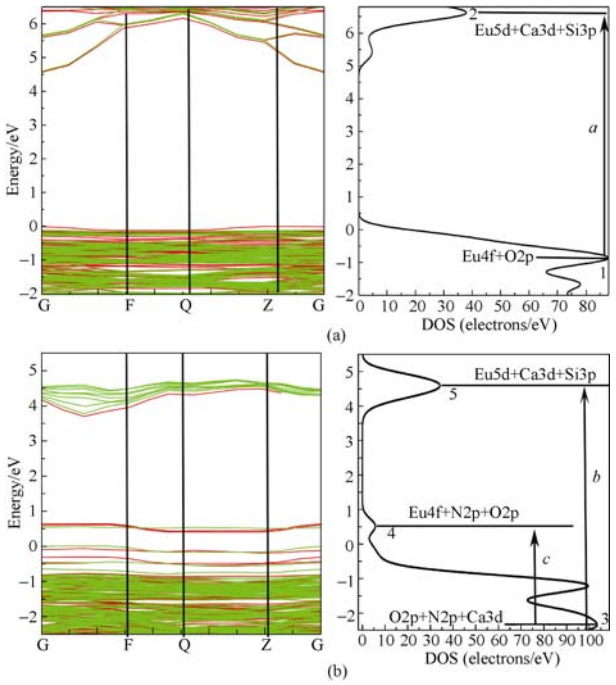

Fig. 2　The band structure and TDOS of Ca_2SiO_4: Eu^{2+} without (a) and with (b) substitution of N atoms for O atoms for the case

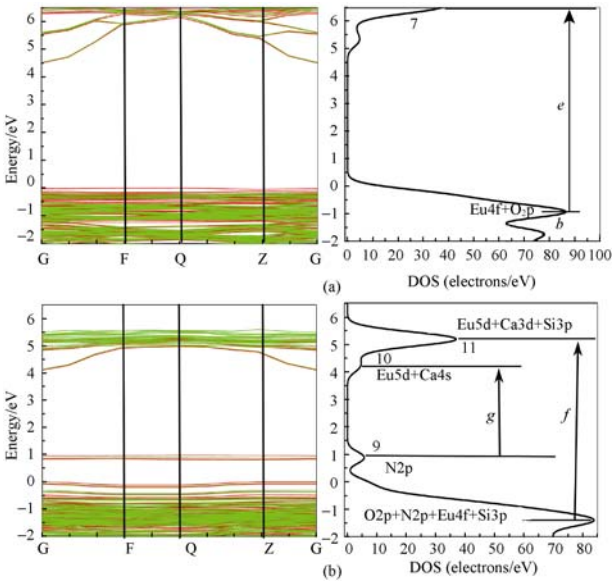

Fig. 3 The band structure and TDOS of Ca_2SiO_4: Eu^{2+} without (a) and with (b) substitution of N atoms for O atoms for the case 2

band gap. For clarity, the Fermi level is set to zero. It is seen from the PDOS of Ca_2SiO_4: Eu^{2+} in Fig. 4(a) that the bottom of the conduction band mainly stems from the hybridized orbits Ca3d and Si3p, while the top of the valence band is mainly composed of the O2p orbital, partly derived from Eu4f. It can be seen from Fig. 4(a) that the band 1 (seen in Fig. 2(a)) with maximum at –0.85 eV mainly originates from O2p state, and band 2 (seen in Fig. 2(a)) with maximum at 6.61 eV mainly stems from Ca3d, Si3p and Eu5d states. When N atoms are doped, the bottom of the conduction band mainly stems from Ca3d, Eu5d and Si3p states, while the top of the valence band is mainly composed of the Eu4f and N2p states. As results, the band 3 (seen in Fig. 2(b)) with maximum at –2.35 eV mainly originates from O2p, N2p and Ca3d states, band 4 (seen in Fig. 2(b)) with maximum at 0.51 eV mainly originates from Eu4f, N2p and O2p states, while band 5 (seen in Fig. 2(b)) with maximum at 4.58 eV is mainly composed of Ca3d, Eu5d and Si2p states. It is seen from Fig. 4(b) that at the Fermi level, N2p orbits and Eu4f orbits overlap each other. The little stabilized electrons at the Fermi level are N2p electrons[17]. Therefore, the energy electron transition is the valence band charges transfer of the nonbonding electron from N2p to the empty band of Eu4f states. Besides, Eu^{2+} ion experiences a strong nephelauxetic effect and crystal field splitting on the 4f orbits.

The PDOS for the N-doped and un-doped β-Ca_2SiO_4: Eu^{2+} for the case 2 are shown in Fig. 5, respectively. It can be seen from the PDOS of Ca_2SiO_4: Eu^{2+} (Fig. 5(a)) that the bottom of the conduction band mainly stems from Ca3d and Si3p states, and the top of the valence band is mainly composed of O2p and Eu4f states, which is similar to the case 1 in Fig. 4(a). The band 6 (seen in Fig. 3(b)) with maximum at –0.94 eV mainly originates from O2p state, and band 7 with maximum (seen in Fig. 3(b)) at 6.55 eV is mainly contributed by Ca3d, Si2p and Eu5d states.

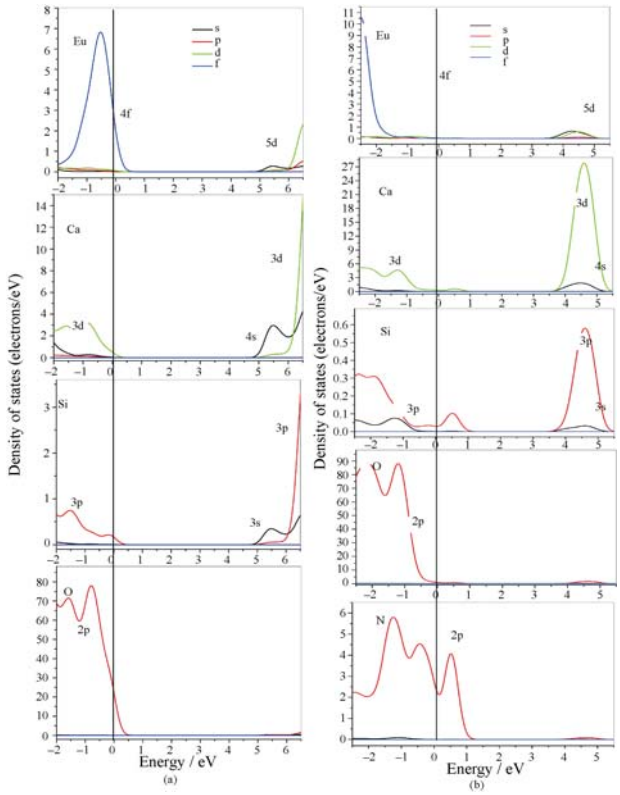

Fig. 4 The PDOS of Ca_2SiO_4: Eu^{2+} without (a) and with (b) substitution of N atoms for O atoms for the case 1

When N atoms are doped in Fig. 5(b), the bottom of the conduction band mainly stems from Ca3d, Eu5d and Si3p states, and the top of the valence band is mainly composed of Eu4f and N2p states, which is similar to the case 1 in Fig. 4(b). Besides, the band 8 (seen in Fig. 3(b)) with maximum at –1.40 eV mainly originates from O2p and Eu4f states, band 9 (seen in Fig. 3(b)) with maximum at 0.88 eV is mainly composed of N2p states, band 10 with maximum at 4.33 eV mainly stems from Ca4s, Eu5d states, and band 11 at 5.20 eV is mainly ascribed to Ca3d, Eu5d states. Thus, N atoms substituted provide many states around the Femi level. It is seen from Fig. 5(b) that N2p, O2p and Eu4f orbits overlap each other around the Fermi level, which results in valence band charges transfer of the electrons from N2p and O2p to the empty band of Eu4f states. Furthermore, as the average bonding length of Ca–O at the Ca(2) sites is smaller than the bonding length of Ca–O at the Ca(1) sites. Thus, Eu^{2+} ions experienced more stronger nephelauxetic effect at the smaller Ca(2) site than it would at the larger Ca(1) site, which results in 5d states splitting into 5d and 5s states in Fig. 5(b).

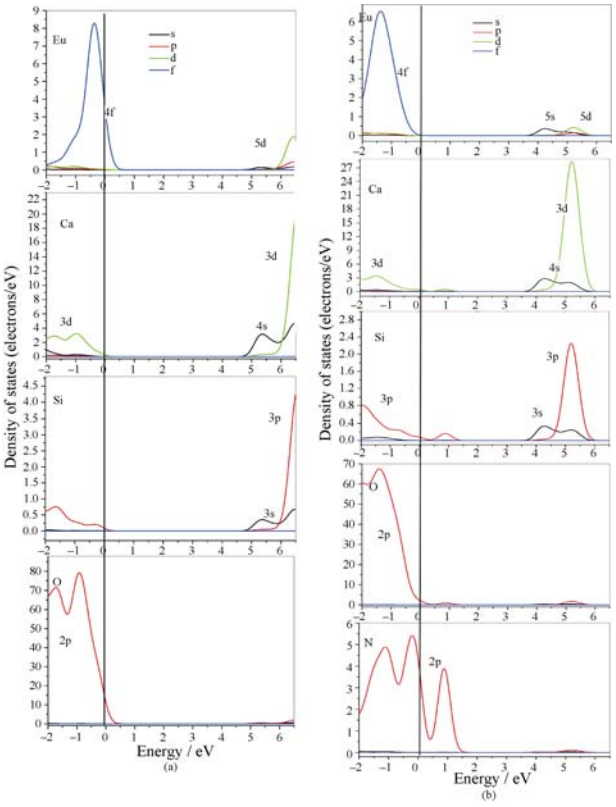

Fig. 5 The PDOS of Ca_2SiO_4: Eu^{2+} without (a) and with (b) substitution of N atoms for O atoms for the case 2

2.3 Absorption spectra

The absorption spectra for the N-doped and un-doped β-Ca_2SiO_4: Eu^{2+} for the case 1 are shown in Fig. 6. Actually, by comparing Fig. 2 and Fig. 4 with Fig. 6, absorption peaks originating from the interband transitions can be easily assigned. It is readily seen from Fig. 6(a) that the short-wavelength absorption peak α about 8 eV in Fig. 6(a) is most readily assigned to the host lattice absorption, *i.e.* O2p to Ca3d interband transition *a*. The absorption spectrum partly matches well with the wavelength range of 220 nm (i.e. 5.64 eV) to 450 nm (i.e. 2.76 eV) attributed to $4f^7 \rightarrow 4f^6 5d$ transition of Eu^{2+} ion[16]. When N atoms are doped, red-shift of absorption spectrum is taken place in Fig. 6(b). Comparing the DOS and absorption spectra, it is seen that the absorption peak β at 6.74 eV, (*i.e.* 184 nm), most readily assigned to the O2p, N2p, Ca3d and Eu4f to Ca3d, Si2p and Eu5d interband transition *b* (marked in Fig. 2(b)), while peak γ at 2.5 eV (*i.e.* 496 nm) is mainly corresponding to the interband transition *c* (marked in Fig. 2(b)) from O2p and N2p to Eu4f. Therefore, the absorption spectra of N-doped Ca_2SiO_4: Eu^{2+} matched well with the wavelength range of 220 nm to 450 nm are attributed to Eu $4f^6 5d \rightarrow 4f^7$ transition. These assignments are summarized in the right panel of Fig. 2. Therefore, the red-shift of absorption spectrum can be attributed to the substitution of N atoms.

Fig. 7 plots the absorption spectra of the N-doped and un-doped β-Ca_2SiO_4: Eu^{2+} phosphors for the case 2. By comparing the total DOS and their absorption spectra, we can see from Ca_2SiO_4: Eu^{2+} in Fig. 7(a) that the short-wavelength absorption peak A at 7.99 eV are mainly corresponding to the transition process *e* (marked in Fig. 3(a)). The absorption spectrum partly matches well with the wavelength range of $4f^7 \rightarrow 4f^6 5d$ transition of Eu^{2+} ions, which results in low green emitting emission intensities.

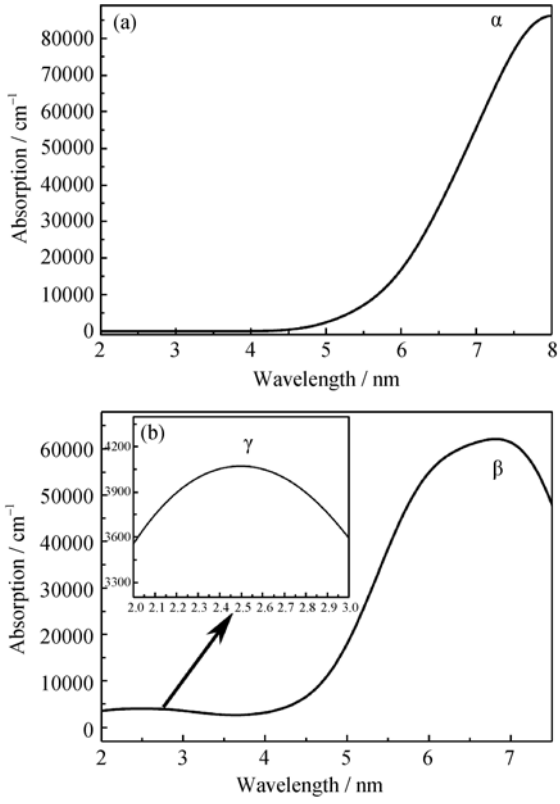

Fig. 6 The absorption spectra of Ca_2SiO_4: Eu^{2+} without (a) and with (b) substitution of N atoms for O atoms for the case 1

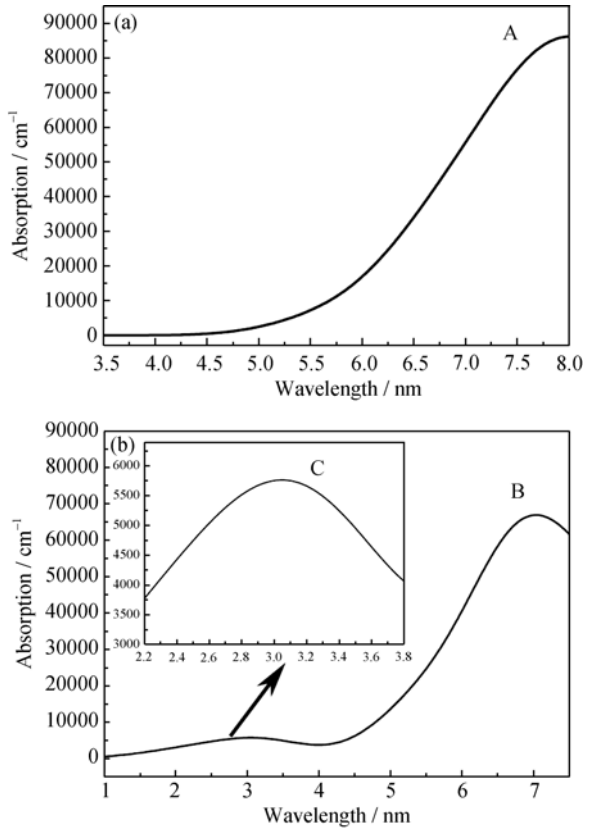

Fig. 7 The absorption spectra of Ca_2SiO_4: Eu^{2+} without (a) and with (b) substitution of N atoms for O atoms for the case 2

As N atoms are doped in Fig. 7(b), a red-shift of theabsorption spectrum is taken place, which is similar to the case 1 in Fig. 6(b). The absorption peak B at 6.94 eV (*i.e.* 178 nm) is most readily assigned to the O2p, N2p, Eu4f and Si3p to Ca3d, Eu5d and Si2p interband transition *f* (marked in Fig. 3(b)), while peak *C* located at 3.06 eV (*i.e.* 405 nm) is mainly corresponding to the N2p to Ca4s and Eu5d interband transition *g* (marked in Fig. 3(b)). As results, the absorption spectra match well with the wavelength range of Eu $4f^65d \rightarrow 4f^7$ transition. It is seen from Fig. 7(b) that absorption spectrum is expended to 500 nm (*i.e.* 2.3 eV), which partly results from the interband transitions originate from N2p to the Eu4f states. Thus, being similar to the case 1, red -shift of absorption spectrum is attributed to the substitution of N atoms.

Therefore, for the $Ca_2SiO_{3.75}N_{0.25}$: Eu^{2+} phosphors, N2p orbits and Eu4f orbits overlap each other at the Fermi level, which leads to the energy electron transition from N2p to Eu4f states. As the average radius of N atoms is smaller than that of O atoms, Eu^{2+} ions experience a strong nephelauxetic effect. As a result, the splitting on the Eu4f and Eu5d states of the phosphors takes place. Therefore, the red-shift of absorption spectrum of N-doped Ca_2SiO_4: Eu^{2+} partly attributes to the shifting up of 4f states and moving down of 5d states. Based on the above reasons, we may forecast that, with increasing N concentration, more overlap of N2p and Eu4f states and stronger splitting on the Eu4f and Eu5d states, which can significantly improve luminescent properties of N-doped Ca_2SiO_4: Eu^{2+}. The relative experiment results can confirm this point[7].

3 Conclusion

To explore the effect of N doping on the Ca_2SiO_4: Eu^{2+} phosphor, the electronic structure and absorption spectrum of N-doped and un-doped Ca_2SiO_4: Eu^{2+} phosphors have been investigated. It has been found that N atoms in silicate matrix provide many states around the Femi level, which leads to elevating the valence band and reducing band gap width. Besides, the interband transition originating from N2p to the Eu4f states partly leads to a red-shift of absorption spectrum. Furthermore, Eu^{2+} ions experience a strong nephelauxetic effect and crystal field due to the coordinating nitrogen ions around the activated centers, which results in Eu4f and 5d states splitting. As results, high absorption bands appears in the wavelength of 220–470 nm, which perfectly match with the radiation of the GaN-based LEDs in the range of 370–450 nm.

Acknowledgements The authors are thankful for the software support by the State Key Laboratory of Polymer materials Engineering of Sichuan University.

References:

[1] YU Q M, LIU Y F, WU S, *et al.* Luminescent properties of Ca_2SiO_4: Eu^{3+} red phosphor for trichromatic white light emitting diodes. *Journal of Rare Earths,* 2008, **26(6):** 783–786.

[2] NAGABHUSHANA H, NAGABHUSHANA B M, KUMAR M M, *et al*. Synthesis, characterization and photoluminescence properties of $CaSiO_3$: Eu^{3+} red phosphor. *Spectrochim Acta A,* 2011, **78(1):** 64–69.

[3] RAO Y, HU X Y, LIU T, *et al.* Pr^{3+}-doped Li_2SrSiO_4 red phosphor for white LEDs. *Journal of Rare Earths,* 2011, **29(3):** 198–201.

[4] YONESAKI Y, TAKEI T, KUMADA N, *et al.* Crystal structure of Eu^{2+}-doped $M_3MgSi_2O_8$ (M: Ba, Sr, Ca) compounds and their emission properties. *Journal of Solid State Chemistry,* 2009, **182(3):** 547–554.

[5] YONESAKI Y, MATSUDA CH. Crystal structure of $Na_2MMgP_2O_8$ (M: Ba, Sr, Ca) orthophosphates and their luminescence properties activated by Eu^{2+}; analogous structural behaviors of glaserite-type phosphates and silicates. *Journal of Solid State Chemistry,* 2011, **184(12):** 3247–3252.

[6] CHOI S, HONG S, KIM J, *et al.* Characterization of Ca_2SiO_4: Eu^{2+} phosphors synthesized by polymeric precursor process. *Journal of the American Ceramic Society,* 2009, **92(9):** 2025–2028.

[7] ZHOU R D, HUANG X F, HUANG W G, *et al.* Preparation and

luminescent properties of $Ca_2Si(O_{4-x}N_x)$: Eu^{2+} green-emitting phosphors. *Acta Phys. Sin.,* 2014, **63:** 197801.

[8] HE ZH, HUANG X F, HUANG W G, *et al.* Synthesis and luminescence properties of a new green emitting $Ca_2MgSi_2O_{7-x}N_x$: Eu^{2+} phosphor. *Journal of Alloys and Compounds,* 2016, **658:** 36-40.

[9] LIAN S, QI Y, RONG C, *et al.* Effectively leveraging solar energy through fersistent dual red phosphorescence: preparation, characterization and density functional theory study of $Ca_2Zn_4Ti_{16}O_{38}$: Pr^{3+}. *Journal of Physical Chemistry C,* 2010, **114(15):** 7196-7204.

[10] TANG J Y, CHEN J H, HAO L Y, *et al.* Green Eu^{2+}- doped $Ba_3Si_6O_{12}N_2$ phosphor for white light-emitting diodes: Synthesis, characterization and theoretical simulation. *Journal of Luminescence,* 2011, **131(6):** 1101–1106.

[11] HINTZE F, JOHNSON N, SEIBALD M, *et al.* Magnesium double nitride Mg_3GaN_3 as new host lattice for Eu^{2+} doping: synthesis, structural studies, luminescence, and band-gap determination. *Chemistry of Materials,* 2013, **25(20):** 4044–4052.

[12] WANG C H, GUI D, QIN R, *et al.* Site and local structure of activator Eu^{2+} in phosphor $Ca_{10-x}(PO_4)_6Cl_2$: xEu^{2+}. *Journal of Solid State Chemistry,* 2013, **206:** 69–74.

[13] QU B, ZHANG B, WANG L, *et al.* Mechanistic study of the persistent luminescence of $CaAl_2O_4$: Eu, Nd. *Chemical Material,* 2015, **27(6):** 2195–2202.

[14] ANISIMOY V I, ZAANEN J, ANDERSEN O K. Band theory and Mott insulators: Hubbard U instead of stoner. *Physical Review B,* 1991, **44(3):** 943.

[15] MONKHORST H J, PACK J D. Special points for Brillouin-zone integrations. *Physical Review B,* 1976, **13:** 5188.

[16] MORI K, KIYANAGI R, YONEMURA M, *et al.* Charge states of Ca atoms in β-Dicalcium silicate. *Journal of Solid State Chemistry,* 2006, **179(11):** 3286–3294.

[17] IBRAHIM I A M, LENCES Z, BENCO L, *et al.* Sm-doped $LaSi_3N_5$: synthesis, computed electronic structure, and band gaps. *Journal of the American Ceramic Society,* 2014, **97(8):** 2546-2551.

氮掺杂对 Ca_2SiO_4: Eu^{2+}电子结构和吸收光谱的影响

陈海涛[1,2], 黄雪飞[1], 黄维刚[1]

(1. 四川大学 材料科学与工程技术学院, 成都 610064; 2. 成都师范学院 物理与工程技术学院, 成都 611130)

摘 要: 运用密度泛函理论研究了氮掺杂对 Ca_2SiO_4: Eu^{2+}电子结构和吸收光谱的影响。研究发现: 氮原子在费米面附近提供了多个态, 从而使荧光粉的带隙宽度变窄, 并导致 N2p 到 Eu4f 的带间能量转移。由于围绕激活中心的氮离子的作用, Eu^{2+} 受到较强的电子云重叠和晶体场影响, 从而造成 Eu4f 和 5d 态的分裂。 因此, 氮掺杂 Ca_2SiO_4: Eu^{2+}的吸收光谱发生了红移, 在 220~470 nm 波长范围内吸收更强。

关 键 词: 氮掺杂; 硅酸盐荧光粉; 发光二极管; 密度泛函理论

中图分类号: O482 **文献标识码:** A